MEASUREMENT OF FURNACE CHARGE TEMPERATURE AND NUMERICAL CALCULATION OF HEAT TRANSFER COEFFICIENT DURING HEATING OF CONTINUOUS CAST PRODUCTS

[1] Martin CHABIČOVSKÝ, [1] Petr KOTRBÁČEK, [2] Petra TUROŇOVÁ

[1]VUT – Brno University of Technology, Brno, Czech Republic, EU, martin.chabicovsky@vut.cz

[2] Třinecké železárny a.s., Třinec, Czech Republic, EU, petra.turonova@trz.cz

https://doi.org/10.37904/metal.2025.5074

Abstract

With rising energy costs, efficient and accurate heating of the charge to rolling temperature is critical to reducing operating costs and improving the quality of the finished product. The surface temperature of the charge obtained from non-contact measurements after exiting the furnace does not provide information about the internal temperature of the charge, nor does it reveal the temperature profile prior to exiting the furnace. As a result, charge overheating, low internal temperature, or insufficient soaking time at target temperature may go undetected. This paper presents a methodology that includes operational temperature measurements inside steel blooms throughout the heating process in industrial furnaces and subsequent numerical calculation of the heat transfer coefficient. The operational measurements were carried out using thermocouples placed inside circular continuously cast semi-finished product, which allowed precise monitoring of the temperature profile throughout the heating process. The data showed that the furnace design significantly affects the thermal homogeneity of the furnace charge. In a rotary hearth furnace, a significant influence of the furnace bottom on the thermal homogeneity of the charge was observed, especially when the bloom was in full contact with the bottom. To better understand these phenomena, a numerical inverse calculation was performed to determine the heat transfer coefficient as a function of position and temperature within the furnace. This coefficient is critical for accurate numerical modelling of the heating process without the need for complex combustion flow and radiative exchange calculations. Knowledge of the heat transfer coefficient allows process optimization, minimization of energy consumption, and improvement of final product quality. The results presented provide valuable insights into industrial practice and demonstrate possible approaches to improve heating efficiency.

Keywords: Heating, temperature measurement, heat transfer coefficient, inverse calculation

1. INTRODUCTION

Accurate and homogeneous heating of continuously cast steel products to rolling temperature is essential to achieve the desired mechanical properties and minimize energy consumption. Standard non-contact surface temperature measurement after the charge exits the furnace does not provide information on the internal temperature distribution or thermal history of the charge. As a result, overheating, inadequate internal heating or insufficient soaking time may go undetected, negatively impacting product quality and process efficiency. The characterization of charge heating by temperature measurement and optimization of furnace energy consumption is described in [1 - 4]. Measurement of charge temperature during heating can be used for inverse calculations [5 - 7] to determine boundary conditions such as heat flux or heat transfer coefficient, which are necessary for accurate numerical simulation of the heating process. These coefficients are critical, especially when modelling without a complex description of combustion and radiation. Wikström et al. used inverse modelling to estimate surface temperatures and heat fluxes during the heating of steel slabs in industrial

furnaces, demonstrating the ability of such models to describe the real heating process [8 and 9]. It follows from work [10] that homogeneous heating is essential for subsequent heat treatment and that thermal inhomogeneity developed during heating can significantly affect the resulting microstructure and final material properties of long steel products.

This paper presents a methodology that combines internal temperature measurements using embedded thermocouples with a simple inverse numerical calculation of the heat transfer coefficient and heat flux. The measurement was carried out during normal industrial operation in a rotary hearth furnace. The calculated boundary conditions are intended for use in numerical simulations and further optimization of the heating process.

2. EXPERIMENTAL MEASUREMENT

The heating of steel blooms (round cast semi-finished products) was measured in the rolling mill. Heating was performed in a large rotary hearth furnace. The heating was measured during normal production. That is, the furnace contained other blooms during the measurement, and the heating was typical.

The bloom with a diameter of 470 mm and a length of 1100 mm was equipped with thermocouples in different positions. The three holes with a diameter of 26.5 mm and a length of 435 mm were drilled in the bloom from the top in the center line. The thread was made in the upper part of the hole to allow good contact of the temperature sensors with the bloom. The sensors were fabricated from the same grade of steel as the bloom. These cylinders were 26.4 mm in diameter and threaded at the top to ensure good contact with the bloom. The sensors had grooves for thermocouples. The measurement point of the thermocouple was precisely bonded to the sensor to ensure good contact with the material. Type K thermocouples, with wires separated by small ceramic tubes to provide good electrical insulation between the wires, especially at temperatures above 1250°C, were used in three sensors. There were two measurement positions (47 mm from top and 47 mm from bottom) in sensors one and three, and three measurement positions (47 mm from top, center (235 mm), and 47 mm from bottom) in Sensor 2. See Figure 1. This represents seven positions within the charge. In addition, the temperature of the atmosphere near the charge was measured at four positions (**Figure 1**, T8 - T11). Two positions (T9 and T10) were 130 mm above the charge and two (T8 and T11) were 120 mm above the bottom of the charge. The data logger, which recorded temperatures every 10 s, was placed in the insulated box connected to the bloom (**Figure 2**). The datalogger remained inside the furnace together with the charge. The photos showing the bloom with the thermocouples and the insulated box with the data logger in the furnace are in **Figure 2.** The other blooms were in the furnace during heating, but there was a gap of about 500 mm from each side of the instrumented bloom, which allowed radiation heating from the sides as well.

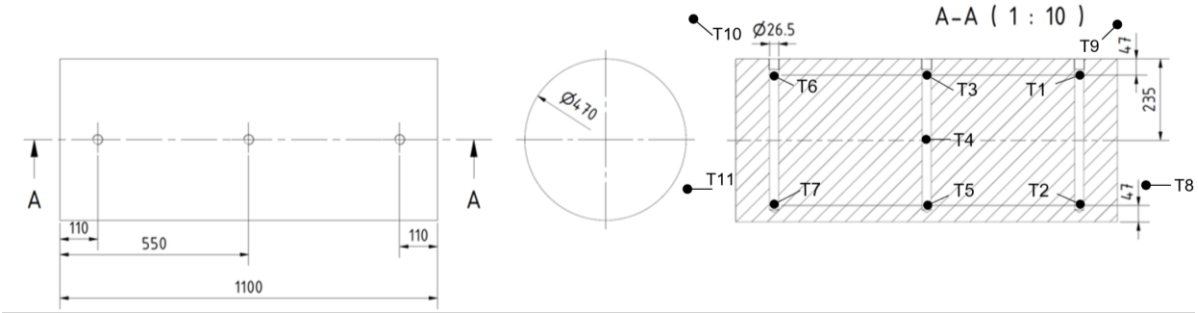

Figure 1 Diagram of the bloom with the positions of the sensors and thermocouples.

Heating took 7 hours and 41 minutes. The bottom of the furnace with the load rotated in small increments as the load passed through six different heating zones. The measured temperatures are shown in **Figure 3**. The details of the thermocouples in Sensor 2 (Thermocouples: T3-T5, center - minimum heat flow along the length of the bloom) for the last two zones are shown in **Figure 4**. These data show a significantly lower temperature

in the lower part of the charge at the end of the heating. The difference between T3 (near the top) and T5 (near the bottom) is 41°C at 460 minutes. It can also be seen that the temperature homogeneity in zone 1 deteriorates due to austenitization. The charge temperature reaches its maximum in the first half of zone 4 and then decreases slightly. The heating of the front part of the charge (T1 and T2) is significantly faster than the middle part due to the additional front surface area.

Figure 2 Bloom with embedded sensors and connected insulated box with data logger (left); cold bloom inserted into furnace (center) and hot bloom removed from furnace (right)

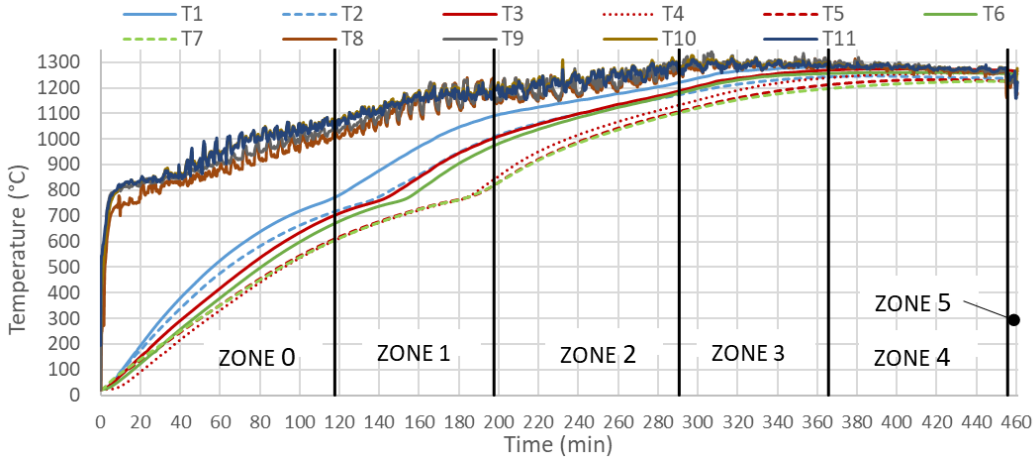

Figure 3 Measured temperatures

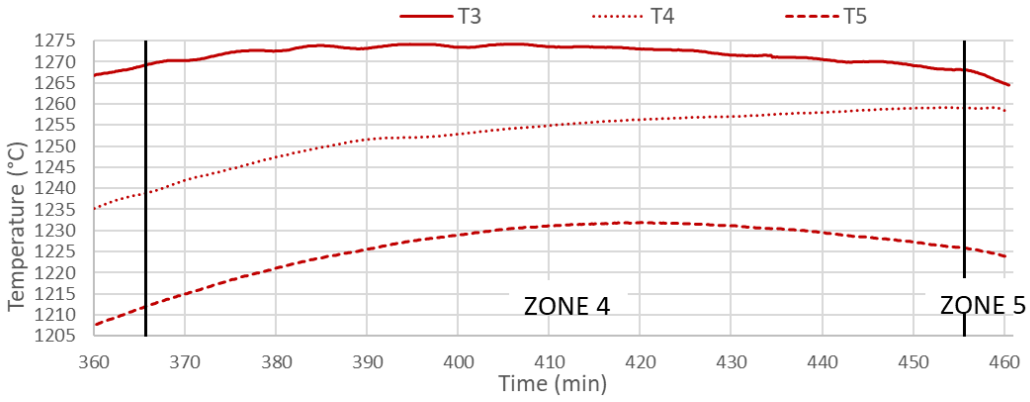

Figure 4 Temperatures measured in the central part of the bloom (T3-T5) - detail of the last two zones

3. INVERSE CALCULATION

The evaluation of the unknown boundary conditions (heat transfer coefficient with surface temperature and surface heat flux) from the measured temperatures was performed using MATLAB software (MathWorks, US) with PDE and optimization toolboxes. The problem was simplified and modeled in 2D, where only the central part of the bloom (sensor 2) was modeled and the heat transfer along the length of the bloom was neglected. Also, only two boundary conditions were applied to the surface: a heat transfer coefficient was applied to the top and side, and a heat flux was applied to the bottom.

The inverse model consisted of the direct solution of a heat transfer problem at each time step with a given forward time step. The boundary conditions were kept constant throughout this direct computation. This was repeated until optimal boundary conditions were found using an optimization technique to minimize the objective function. This was repeated for each step. The minimization was performed separately for heat transfer coefficient (thermocouple T3) and heat flux (thermocouple T5) at a given time. The objective function was minimized using a function fminbnd (a combination of golden section and parabolic interpolation methods). The objective function was:

$$SSE = \sum_{i=m+1}^{m+n} \left(T_i^{measured} - T_i^{computed}\right)^2, \quad (1)$$

where *m* is the time at which the boundary condition is computed, and *n* is the number of future time steps.

The PDE toolbox, which uses quadratic element FEM to solve partial differential equations, was used for the direct heat transfer calculation. The mesh scheme and applied boundary conditions are shown in **Figure 5** (left), the maximum element size was set to 20 mm and the element size (edge length) on the surface was 5 mm. The inverse calculation was performed with future time 270 s (which provided stable and sufficient resolution of results) and with variable time step (90 seconds, near austenitization (100 - 250 min) 20 s). The heat flux was applied to the bottom part (angle of 25°), the perfect insulation was applied in the symmetry axis and the rest was a heat transfer coefficient. The ambient temperature in Newton's boundary condition was estimated from thermocouples T9 and T10 (above the top surface) by interpolation to the position of sensor 2 and was significantly smoothed. The thermophysical properties used in the model are shown in Figure 5 (right). The density was temperature independent, and its value was 7748.68 kg m^{-3}. The initial estimation of the boundary conditions was performed with thermophysical properties measured directly using the Flash Line method (Flash Line TM 4010, Anter corporation, US).

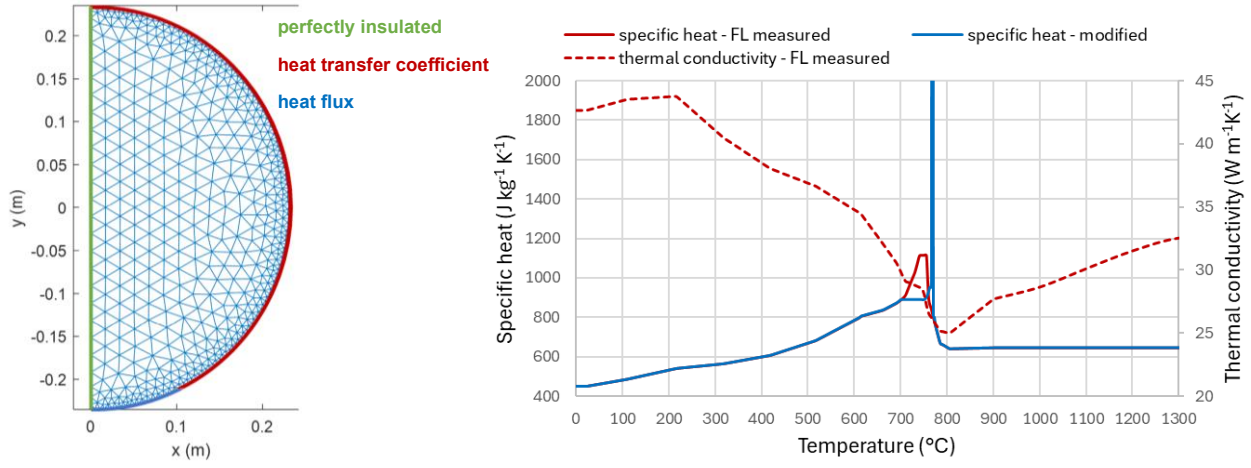

Figure 5 Mesh with marked positions of boundary conditions (left), thermophysical properties used in the model (right)

The results (**Figure 6**, marked by _FL) were not good at times (100 - 230 min) when the transformation to austenite occurred. There was a significant drop in the calculated boundary conditions between these times. The specific heat was modified around the austenitization temperature (peak specific heat is 35 kJ kg^{-1} K^{-1} at 768 °C) to better fit realistic values of boundary conditions around the phase change. See **Figure 5** (right) and **Figure 6**. This helped significantly, but for a better result in times near austenitization, the correct value of the latent heat and a better application of the phase change in the model is needed. The comparison of calculated and measured temperatures is shown in **Figure 7** and the calculated temperature field at times 242 minutes and 455 minutes is shown in **Figure 8**. The accuracy of the heat transfer coefficient estimation may be worse from about 380 minutes due to the very small temperature difference between the surface and ambient temperature and the uncertainty in the measurement. The significant heat loss from the bottom surface is visible from 250 minutes.

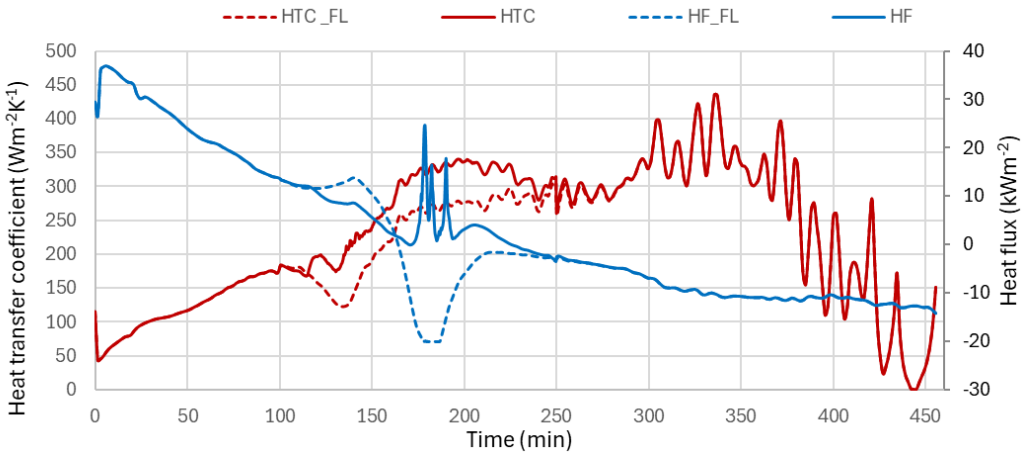

Figure 6 Calculated heat transfer coefficient (HTC) and heat flux (HF) for measured (_FL) and modified thermophysical properties

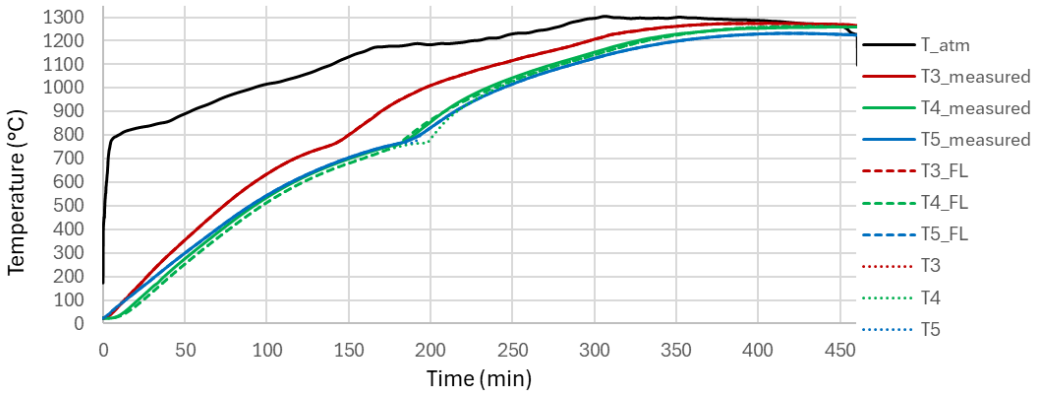

Figure 7 Comparison of measured (solid lines, T3, T4, T5, and T_atm) and calculated temperatures for measured (dashed lines, _FL) and modified (dotted lines) thermophysical properties

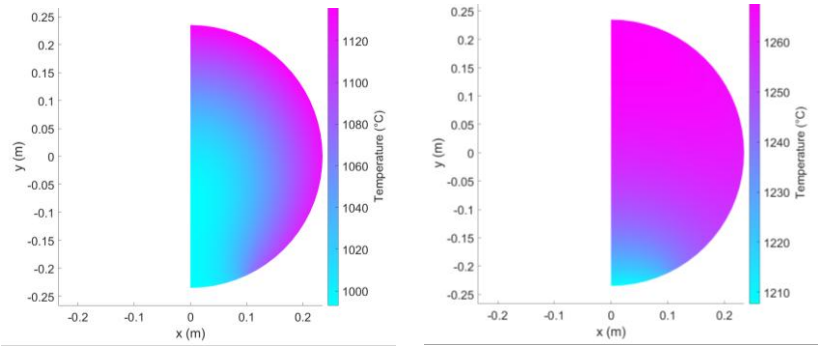

Figure 8 Temperature field at times 242 min (left) and 455 min (right) for modified thermophysical properties

4. CONCLUSION

The presented methodology allows accurate determination of internal temperature profile and boundary conditions (heat flux and heat transfer coefficient) during charge heating. The results confirm the significant influence of the furnace design on thermal homogeneity, especially due to the bottom contact heat losses. The calculated boundary conditions can be directly used in numerical simulations of the heating process, allowing its optimization in terms of energy consumption and product quality.

ACKNOWLEDGEMENTS

The paper presented has been supported by the internal grant of the Brno University of Technology focused on specific research and development No. FSI-S-23-8254.

REFERENCES

[1] JANG, Jiin-Yuh, HUANG, Jun-Bo. Optimization of a slab heating pattern for minimum energy consumption in a walking-beam type reheating furnace. *Applied Thermal Engineering*. 2015, vol. 85, pp. 313–321. https://doi.org/10.1016/j.applthermaleng.2015.04.029

[2] JANG, Jung Hyun, LEE, Dong Eun, KIM, Man Young, KIM, Hyong Gon. Investigation of the slab heating characteristics in a reheating furnace with the formation and growth of scale on the slab surface. International *Journal of Heat and Mass Transfer*. 2010, vol. 53, no. 19–20, pp. 4326–4332. https://doi.org/10.1016/j.ijheatmasstransfer.2010.05.061

[3] EMADI, Ali, SABOONCHI, Ahmad, TAHERI, Mahdi, HASSANPOUR, Saeid. Heating characteristics of billet in a walking hearth type reheating furnace. *Applied Thermal Engineering*. 2014, vol. 63, no. 1, pp. 396–405. https://doi.org/10.1016/j.applthermaleng.2013.11.003

[4] GOŁDASZ, Andrzej, MALINOWSKI, Zbigniew, CEBO-RUDNICKA, Agnieszka. Thermomechanical analysis of the charge heating in a rotary furnace. *Archives of Metallurgy and Materials*. 2019, vol. 64, no. 4, pp. 1377–1384. https://doi.org/10.24425/amm.2019.130104

[5] BECK, James V., BLACKWELL, Ben, ST. CLAIR JR., Charles H. Inverse Heat Conduction: Ill-posed Problems. New York: Wiley, 1985.

[6] POHANKA, M., WOODBURY, K. A. A Downhill Simplex method for computation of interfacial heat transfer coefficients in alloy casting. *Inverse Problems in Engineering*. 2003. vol. 11, pp. 409-424. https://doi.org/10.1080/1068276031000109899

[7] MALINOWSKI, Zbigniew, CEBO-RUDNICKA, Agnieszka, HADAŁA, Błażej, et al. Implementation of one and three-dimensional models for heat transfer coefficient identification over the plate cooled by the circular water jets. *Heat and Mass Transfer*. 2018, vol. 54, pp. 2195–2213. https://doi.org/10.1007/s00231-017-2195-0

[8] WIKSTRÖM, Patrik, BLASIAK, Wlodzimierz, BERNTSSON, Fredrik. Estimation of the transient surface temperature, heat flux and effective heat transfer coefficient of a slab in an industrial reheating furnace by using

an inverse method. *Steel Research International*. 2007, vol. 78, no. 1, pp. 63–70. https://doi.org/10.1002/srin.200705861

[9] WIKSTRÖM, Patrik, BLASIAK, Wlodzimierz, BERNTSSON, Fredrik. Estimation of the transient surface temperature and heat flux of a steel slab using an inverse method. Applied Thermal Engineering. 2007, vol. 27, no. 14–15, pp. 2463–2472. https://doi.org/10.1016/j.applthermaleng.2007.02.005

[10] KOTRBÁČEK, Petr, CHABIČOVSKÝ, Martin, RESL, Ondřej, KOMÍNEK, Jan, LUKS, Tomáš. The efficient way to design cooling sections for heat treatment of long steel products. *Materials*. 2023, vol. 16, no. 11, p. 3983. https://doi.org/10.3390/ma16113983